

SHAPE EVOLUTION OF A SUBLIMING SURFACE SUBJECTED TO UNSTEADY SPATIALLY NONUNIFORM HEAT FLUX

F. W. SPAID*, A. F. CHARWAT†, L. G. REDEKOPP‡ and R. ROSEN§

University of California, Los Angeles, California, U.S.A.

(Received 22 January 1970 and in revised form 15 July 1970)

Abstract—An investigation of two-dimensional, unsteady heat conduction in a solid with phase change at an exposed boundary has been conducted, including a perturbation analysis and numerical computations. The zero-order solution from which the perturbation analysis was developed is the steady, one-dimensional recession of a solid slab in response to a uniform heat input. The analysis has been carried out for small values of $(\delta/b)^2$, where δ is the characteristic length for the temperature distribution in the solid, and b is the length scale of the lateral nonuniformity of the heat flux.

A finite-difference analog of the governing equations was programmed, for the purpose of providing results for large nonuniformity in both heat flux and surface shape. Sample results are presented for two types of heat inputs: (a) one in which the spatial variation was sinusoidal, and (b) one which consisted of two constant levels connected by a half-wave cosine transition. Good agreement was obtained between predictions of the first-order analysis and results of the numerical computation for small times. For relatively large values of time, the computed surface shapes were found to become self-preserving. In case (a) groove shapes and depths tended to become time-independent, and in case (b), a straight ramp of constant slope tended to form. The mass loss of the solid was found to be smaller when the slab was subject to spatially uniform heating than when it was heated uniformly with the same average intensity (when lateral conduction was not neglected). For a given heating, the mass loss with lateral conduction was always less than when lateral conduction was neglected.

An empirical correlation of the numerical results shows surface slopes or grooves depths to be proportional to a length scale which is associated with the nonuniformity in the heat flux, and its magnitude. The characteristic time for the appearance of surface features is $(\delta b)/\alpha$, where α is the thermal diffusivity of the solid.

NOMENCLATURE

b ,	length scale of lateral heat flux gradients;	H ,	reference length based upon steady, one-dimensional recession, equation (39);
c_p ,	specific heat;	j ,	time index;
d ,	lateral half-width of the body;	k ,	thermal conductivity;
F ,	dimensionless heat flux function;	L ,	heat of sublimation;
ΔF ,	$F_{\max} - F_{\min}$;	m ,	lateral coordinate index;
		M ,	maximum value of m ;
		n ,	vertical coordinate index;
		p ,	Laplace transform variable;
		Q ,	heat flux per unit area per unit time;
		s ,	surface position coordinate;
		S ,	dimensionless surface position coordinate, equation (8);
		\mathcal{S} ,	dimensionless mass-loss function, equation (38);

* Assistant Professor of Engineering, University of California, Los Angeles, California.

† Professor of Engineering, University of California, Los Angeles, California.

‡ Research Assistant; now Assistant Professor, Department of Aerospace Engineering, University of Southern California, Los Angeles, California.

§ Senior Engineer/Scientist, McDonnell Douglas Astronautics Company, Western Division, Huntington Beach, California.

t ,	dimensional temperature ;
t_s ,	dimensional sublimation temperature ;
t_0 ,	slab temperature for $y \rightarrow \infty$;
T ,	dimensionless temperature, equation (8) ;
U ,	dimensionless temperature used in the numerical analog ;
V ,	dimensionless temperature used in the numerical analog ;
x ,	lateral coordinate ;
y ,	vertical coordinate ;
z ,	transformed vertical coordinate, equation (7) ;
α ,	thermal diffusivity ;
β ,	sublimation parameter, equation (8) ;
γ ,	thermal aspect ratio, equation (8) ;
δ ,	thermal penetration depth, equation (8) ;
η ,	dimensionless vertical coordinate (z/δ) ;
ξ ,	dimensionless lateral coordinate (x/b) ;
θ ,	dimensional time ;
ρ ,	mass density ;
λ_1, λ_2 ,	functions derived from solution of equation (18a), see equations (20) and (22) ;
τ ,	dimensionless time variable, equation (8) ;
$\Delta\tau$,	dimensionless time increment ;
$\Delta\eta$,	dimensionless vertical distance increment ;
$\Delta\xi$,	dimensionless lateral distance increment.

I. INTRODUCTION

HEAT transfer to a body with phase change at the exposed boundaries (sometimes referred to as Stefan's Problem) has attracted the attention of numerous investigators over the past century. Recently the development of ablative heat sinks for thermal protection of hypersonic vehicles has given the problem considerable impetus, but there are also other less publicized applications of considerable interest. For instance, the problem of the melting of polar ice-caps was

one that stimulated the present study.

The first important exact solution to a phase change problem was given by Neumann in 1860 [1]. He considered the solidification of a semi-infinite slab existing initially in the liquid state at constant temperature $t_0 > 0$. For all times $\theta > 0$, the exposed surface ($y = 0$) was maintained at a temperature $t = 0$, and the location of the solid-liquid interface was determined as a function of time. The solution satisfying conditions for all time was found to be $s(\theta) \sim \sqrt{\theta}$. Various other solutions have subsequently appeared in the literature and are discussed in the excellent reviews by Muehlbauer and Sunderland [2], by Boley [3], and by Bankoff [4]. The special difficulty associated with the phase change problem is the non-linearity introduced by the existence of a moving boundary. This requires that special solutions be obtained for each different set of boundary conditions. These difficulties are compounded by the nonexistence of similarity conditions for situations of an arbitrary heat flux on the moving boundary or of an arbitrary initial temperature distribution within the body.

Nearly all of the previous work has been done for one-dimensional cases where conditions are laterally uniform or where the influence of lateral temperature gradients and surface heat flux nonuniformities is neglected. The only two-dimensional treatment known to the authors is the analytic solution given by Boley and Sikarskie [5] for the initial sublimation rate of a semi-infinite strip under a spatially varying ($Q(x) \sim \cos x$) heat flux. The essential feature of their method of analysis is that it deals mathematically with a fictitious body, whose shape is unchanged and is identical with that of the body before any phase transformation occurs. The fictitious body is exposed to an imaginary heat flux whose magnitude is adjusted so that it satisfies the appropriate interface conditions. In this formulation the original boundary value problem is replaced by an ordinary integro-differential equation which was solved in series form, with results obtained for the

leading terms in the series. However, the surface recession history for long sublimation times and for realistic surface heat transfer distributions has not been examined. It is the objective of this effort to study surface recession histories when the incident heat flux is spatially nonuniform and nonsteady, and to evaluate the role of lateral conduction.

II. FORMULATION OF THE PROBLEM

The equation describing unsteady, two-dimensional heat conduction in a body with temperature-independent physical properties is

$$\frac{\partial t}{\partial \theta} = \alpha \left(\frac{\partial^2 t}{\partial x^2} + \frac{\partial^2 t}{\partial y^2} \right). \quad (1)$$

This equation is to be solved subject to the following initial and boundary conditions. The initial temperature distribution within the body, and the initial shape of the surface are prescribed:

$$t(x, y, 0) = t_i(x, y) \quad (2a)$$

$$s(x, 0) = s_i(x). \quad (2b)$$

The initial recession rate must be consistent with the energy balance at the exposed boundary. Boundary conditions for the problem are

$$t(x, y, \theta) = t_\infty \quad \text{as } y \rightarrow \infty \quad (3a)$$

(infinite slab in the direction normal to the surface) and

$$\frac{\partial t}{\partial x} = 0 \quad \text{at } x = \pm d \quad (3b)$$

(insulated lateral boundaries at $x = \pm d$). An additional condition is obtained from an energy balance at the exposed surface, the simplest form of which is

$$Q_n(x, \theta) = -k \left. \frac{\partial t}{\partial n} \right|_s + \dot{m}L, \quad (4)$$

where $Q_n(x, \theta)$ is the component of heat flux normal to the local surface. For the sake of convenience, (4) is rewritten in terms of the incident heat flux per unit area and time, $Q(x, \theta)$,

normal to a plane $y = \text{constant}$.

$$Q(x, \theta) = -k(-t_x s_x + t_y) \Big|_{y=s(x, \theta)} + (1 + s_x^2) \rho L \dot{s}, \quad (5)$$

where subscripts denote differentiation. This relation models a radiant heat input independent of the instantaneous surface shape. If convective heat- and mass-transfer coupling were included, an additional term would be added accounting for the heat blockage effect introduced by the blowing at the gas-solid interface. Also, the surface shape would be coupled with the heat input function because of its influence on the nature of the boundary layer.

Coupled with the energy balance (5), one must make a statement regarding the phase change kinetics. For simplicity, a fixed sublimation temperature is used here. This condition is

$$\left. \begin{aligned} \dot{s} &= 0 & \text{when } t(x, s, \theta) < t_s \\ \dot{s} &> 0 & \text{when } t(x, s, \theta) = t_s, \end{aligned} \right\} \quad (6)$$

where the magnitude of s is computed from (5) and t_s is prescribed.

Statement (6) together with relation (5) is sufficient to completely describe the boundary condition at the exposed moving surface.

The preceding is a formulation in terms of fixed coordinates (x, y) wherein the exposed surface moves relative to the coordinate axes. Inherent in this formulation is the difficulty of applying boundary condition (5) at the *a priori* unknown location $s(x, \theta)$. In certain circumstances this difficulty can be avoided by transforming to a coordinate system moving with the receding boundary. This type of transformation in phase change problems was first introduced by Landau [6] for the case of one-dimensional conduction in a slab with uniform incident heat flux. In this spirit we introduce the coordinate transformation

$$z = y - s(x, \theta), \quad x = x, \quad (7)$$

as illustrated in Fig. 1. It is to be emphasized,

however, that the difficulties associated with the existence of a moving boundary will not be eliminated by working in the transformed (x, y) plane. The undesirable problem of applying a boundary condition at an unknown position is avoided at the expense of transferring the essential nonlinearity of the problem directly to the governing partial differential equation for the temperature field within the body. In view of the numerical solutions to be obtained subsequently, it was thought advisable to work in the transformed (x, z) plane rather than the (x, y) plane in order to avoid the complications which arise from the motion of a boundary across a grid lattice.

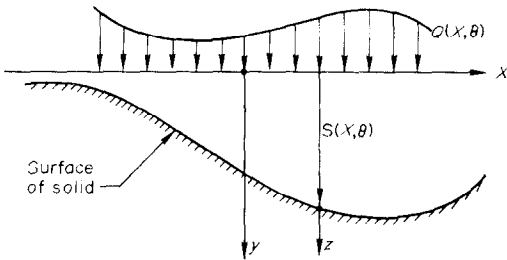


FIG. 1. Definitions of coordinate systems.

Applying the transformation (7) to the foregoing set of equations and simultaneously introducing the nondimensional quantities

$$\begin{aligned} \xi &= \frac{x}{b}, & \eta &= \frac{z}{\delta}, & \tau &= \frac{\theta x}{\delta^2}, & S &= \frac{s}{\delta}, \\ d' &= \frac{d}{b}, & T &= \frac{t - t_0}{t_s - t_0}, & \gamma &= \frac{\delta}{b}, \\ \beta &= \frac{c_p(t_s - t_0)}{L}, & \text{and } \delta &= \frac{\rho \alpha L}{Q_0}. \end{aligned} \quad (8a)$$

with the heat input represented by

$$\frac{Q}{Q_0} = F(\xi, \tau), \quad (8b)$$

the partial differential equation (1) becomes

$$T_\tau = (S_\tau - \gamma^2 S_{\xi\xi}) T_\eta + (1 + \gamma^2 S_\xi^2) T_{\eta\eta} + \gamma^2 (T_{\xi\xi} - 2S_\xi T_{\xi\eta}), \quad (9)$$

where subscripts denote differentiation. The transformed boundary conditions are

$$T(\xi, \eta, \tau) = 0 \quad \text{as } \eta \rightarrow \infty \quad (10a)$$

and

$$T_\xi = 0 \quad \text{at } \xi = \pm d', \quad (10b)$$

the latter condition applying if the body is bounded laterally by installed walls at $\xi = \pm d'$. Writing the surface boundary condition in terms of the transformed variables yields

$$F(\xi, \tau) = -\beta [-\gamma^2 S_\xi T_\xi + (1 + \gamma^2 S_\xi^2) T_{\eta\xi}]_{\xi, 0, \tau} + (1 + \gamma^2 S_\xi^2) S_\tau. \quad (11)$$

Coupled with this relation is the phase change law which transforms to

$$S_\tau = 0 \quad \text{when } T(\xi, 0, \tau) < 1$$

and

$$S_\tau > 0 \quad \text{when } T(\xi, 0, \tau) = 1.$$

$$T(\xi, 0, \tau) \leq 1.$$

The initial conditions consist of the specification of an initial surface shape and temperature field and application of the surface boundary condition (11) at $\tau = 0$. The scaling quantities $t_s - t_0$ and Q_0 are introduced to make the functions T and F of order unity.

The quantity δ defined in (8) is a measure of the thermal penetration depth resulting from a uniform steady heat input rate of magnitude Q_0 applied at the surface of a body with physical properties ρ , α and L , and is obtained from the solution for steady, one-dimensional recession. The quantity b is a length characterizing the lateral scale of the spatial nonuniformity in the incident heat flux. The use of these two parameters to nondimensionalize the normal and lateral derivatives, respectively, has essentially stretched the respective coordinates in the (ξ, η) plane such that gradients of the dependent variables are of equal importance. As a consequence of the use of two characteristic lengths in the nondimensionalization, a thermal aspect-ratio parameter γ appears in the equations. It is clear that

if the spatial gradients of the applied heat flux (scaled by b) are of the same order as the thermal penetration depth (scaled by δ), that is, when γ is of order unity, lateral conduction is significant and cannot be neglected in determining the surface recession rate.

Because of the nonlinear nature of equation (9) and since there exists no similarity variable to reduce it to an ordinary differential equation, two methods of solution have been utilized. The first is a perturbation analysis. The second approach is a finite-difference solution of the problem which was used to obtain numerical solutions for several different sets of initial and boundary conditions.

III. PERTURBATION ANALYSIS

When the incident heat flux is nearly uniform over the surface of the body, the thermal aspect ratio γ becomes very small. The parameter γ appears in the equations as γ^2 . This suggests an expansion of variables in terms of this small parameter:

$$\begin{aligned} T &= T^{(0)}(\eta, \tau) + \gamma^2 T^{(1)}(\xi, \eta, \tau) \\ &\quad + \gamma^4 T^{(2)}(\xi, \eta, \tau) + \dots, \\ S &= S^{(0)}(\tau) + \gamma^2 S^{(1)}(\xi, \tau) \\ &\quad + \gamma^4 S^{(2)}(\xi, \tau) + \dots, \text{ and} \\ F &= 1 + \gamma^2 F^{(1)}(\xi, \tau) + \gamma^4 F^{(2)}(\xi, \tau) + \dots \end{aligned} \quad (13)$$

For simplicity, we restrict the analysis to the class of problems for which the surface is initially flat, $S(0) = S_\xi(\xi, 0) = S_{\xi\xi}(\xi, 0) = 0$ and all higher order terms in T, S and F , are zero for $\tau < 0$. Physically, this means that for $\tau < 0$ there is steady recession of a slab in response to a spatially uniform, steady heat input. At $\tau = 0$, a spatially varying perturbation is added to the heat input function. Substituting the expansions for T, S and F , into the differential equation (9) and the initial and boundary conditions given in equations (10), (11a) and (12), terms of zero order yield

$$\begin{aligned} T_\eta^{(0)} - S_\tau^{(0)} T_\eta^{(0)} - T_{\eta\eta}^{(0)} &= 0, \\ S^{(0)}(0) &= 0, \end{aligned}$$

$$\begin{aligned} T^{(0)}(\eta, \tau) &= 0 \text{ as } \eta \rightarrow \infty, \\ T^{(0)}(0, \tau) &= 1, \text{ and} \\ 1 &= -\beta T_\eta^{(0)}(0) + S_\tau^{(0)}. \end{aligned} \quad (14)$$

The zero-order solution is

$$T^{(0)} = \exp(-S_\tau^{(0)}\eta) \quad (15)$$

with

$$S_\tau^{(0)} = \frac{1}{\beta + 1}.$$

Terms of order γ^2 yield

$$T_\tau^{(1)} - S_\tau^{(0)} T_\eta^{(1)} - T_{\eta\eta}^{(1)} = S_\tau^{(1)} T_\eta^{(0)}, \quad (16a)$$

$$\begin{aligned} T^{(1)}(\eta, 0) = T^{(1)}(0, \tau) = T^{(1)}(\infty, \tau) \\ = S^{(1)}(0) = 0, \text{ and} \end{aligned} \quad (16b)$$

$$F^{(1)}(\xi, \tau) = -\beta T_\eta^{(1)}(0) + S_\tau^{(1)}. \quad (16c)$$

Terms of order γ^4 yield

$$\begin{aligned} T_\tau^{(2)} - S_\tau^{(0)} T_\eta^{(2)} - T_{\eta\eta}^{(2)} = S_\tau^{(1)} T_\eta^{(1)} \\ + (S_\tau^{(2)} - S_{\xi\xi}^{(1)}) T_\eta^{(0)} - T_{\xi\xi}^{(1)}, \end{aligned} \quad (17a)$$

$$\begin{aligned} T^{(2)}(\eta, 0) = T^{(2)}(0, \tau) = T^{(2)}(\infty, \tau) \\ = S^{(2)}(0) = 0, \text{ and} \end{aligned} \quad (17b)$$

$$F^{(2)} = -\beta T_\eta^{(2)} + S_\tau^{(2)}. \quad (17c)$$

The Laplace transform of equations (16) (transformed variables are denoted by an asterisk) after substitution for $T_\eta^{(0)}$ from (15) is

$$\begin{aligned} p T^{(1)*} - S_\tau^{(0)} T_\eta^{(1)*} - T_{\eta\eta}^{(1)*} \\ = S_\tau^{(1)*} S_\tau^{(0)} \exp(-S_\tau^{(0)}\eta), \text{ and} \end{aligned} \quad (18a)$$

$$F^{(1)*} = -\beta T_\eta^{(1)*}(0) + S_\tau^{(1)*}. \quad (18b)$$

The solution for the transformed temperature field, which may be obtained by Green's function techniques, is

$$\begin{aligned} T^{(1)*} &= \frac{S_\tau^{(1)*} S_\tau^{(0)}}{p} \\ &\times [\exp(-\lambda_2 \eta) - \exp(-S_\tau^{(0)}\eta)], \end{aligned} \quad (19)$$

where

$$\lambda_2 = \frac{S_\tau^{(0)}}{2} + \sqrt{\left(p + \frac{S_\tau^{(0)2}}{4}\right)}. \quad (20)$$

The boundary condition corresponding to the energy balance at the surface has not yet been satisfied. It is possible to solve an inverse problem by specifying $S_\tau^{(1)}$ and determining the corresponding value of $F^{(1)*}$ from equation (18b). A direct solution which is valid for small values of time can be obtained by differentiating equation (19) and substituting into (18b), which gives

$$S_\tau^{(1)} = \frac{F^{(1)*}}{1 + \beta S_\tau^{(0)} \lambda_1}, \quad (21)$$

where

$$\lambda_1 = -\frac{S_\tau^{(0)}}{2} + \sqrt{\left(p + \frac{S_\tau^{(0)2}}{4}\right)}. \quad (22)$$

The first-order heat input function $F^{(1)}$ may be expanded as a power series in τ ,

$$F^{(1)} = F_0^{(1)}H(\tau) + F_1^{(1)}\tau + F_2^{(1)}\tau^2 + \dots, \quad (23)$$

where $H(\tau)$ is the Heaviside unit function. If we substitute the Laplace transform of this expansion into equation (21) and expand the result as a power series in p^{-1} , we have

$$\begin{aligned} S_\tau^{(1)*} &= F_0^{(1)}p^{-1} - F_0^{(1)}\frac{\beta}{\beta+1}p^{-3/2} \\ &+ \left[F_0^{(1)}\frac{\beta(\beta+\frac{1}{2})}{(\beta+1)^2} + F_1^{(1)} \right] p^{-2} - \frac{\beta}{\beta+1} \left[F_0^{(1)} \right. \\ &\times \left. \frac{(\beta^2 + \beta + \frac{1}{8})}{(\beta+1)^2} + F_1^{(1)} \right] p^{-5/2} + \left\{ \frac{\beta}{(\beta+1)^2} \right. \\ &\times \left. \left[F_0^{(1)}\frac{\beta(\beta+\frac{1}{2})}{\beta+1} + F_1^{(1)}(\beta+\frac{1}{2}) \right] \right. \\ &\left. + 2F_2^{(1)} \right\} p^{-3} + O(p^{-7/2}). \quad (24) \end{aligned}$$

This expression can be inverted term-by-term yielding

$$\begin{aligned} S_\tau^{(1)} &= F_0^{(1)} - \frac{2\beta}{\beta+1} F_0^{(1)} \sqrt{\left(\frac{\tau}{\pi}\right)} + \left[F_0^{(1)} \right. \\ &\left. \frac{\beta(\beta+\frac{1}{2})}{(\beta+1)^2} + F_1^{(1)} \right] \tau - \frac{\beta}{\beta+1} \left[F_0^{(1)} \right. \end{aligned}$$

$$\begin{aligned} &\times \left. \frac{(\beta^2 + \beta + \frac{1}{8})}{(\beta+1)^2} + F_1^{(1)} \right] \frac{4\tau^{3/2}}{3\sqrt{\pi}} + \frac{\beta}{\beta+1} \\ &\times \left\{ \frac{\beta}{(\beta+1)^2} \left[F_0^{(1)}\frac{\beta(\beta+\frac{1}{2})}{\beta+1} + F_1^{(1)}(\beta+\frac{1}{2}) \right] \right. \\ &\left. + 2F_2^{(1)} \right\} \frac{\tau^2}{2} + O(\tau^{5/2}). \quad (25) \end{aligned}$$

The restriction of the first-order solution to small values of τ [equation (23)] is not particularly severe, since for most classes of problems this is already implied by the requirement that the perturbation of the initial surface shape be small [equation (13)]. For τ approaching zero, the surface recession rate is given to order γ^2 by

$$S_\tau = \frac{1 + \gamma^2 F_0^{(1)}}{\beta+1} + \frac{\beta\gamma^2 F_0^{(1)}}{\beta+1} + O(\tau^{1/2}). \quad (26)$$

The first term in equation (26) is exactly the steady-state recession rate corresponding to the perturbed heat input. S_τ is thus initially larger than the steady-state value. The conduction process associated with a characteristic time is long compared to the instantaneous increase in F at $\tau = 0$. As a result, conduction initially has no effect, and the increased heat input is reflected entirely in vaporization of the surface material.

It is interesting to note that the problem which we have posed, to first order in γ^2 , corresponds to a one-dimensional unsteady problem. Therefore, the results can be applied to a situation in which the initial surface is not flat by adding $S_i(\xi)$ to surface shapes obtained by integrating (25).

It is possible to use the solution for $S_\tau^{(1)}$ to obtain a first-order solution for the temperature field. If equation (24) is substituted into equation (19) and the result is expanded in a power series in p^{-1} and inverted term-by-term, the first few terms in the expansion for the temperature field are

$$T^{(1)} = \frac{F_0^{(1)} \exp[-\eta/2(\beta+1)]}{\beta+1} \left\{ \left(\tau + \frac{\eta^2}{2} \right) \right.$$

$$\begin{aligned} & \times \operatorname{erfc}\left(\frac{\eta}{2\sqrt{\tau}}\right) - \eta\sqrt{\left(\frac{\tau}{\pi}\right)} \exp(-\eta^2/4\tau) \\ & + \left[\frac{\eta}{8(\beta+1)^2} + \frac{\beta}{\beta+1}\right] (4\tau)^{3/2} \int_{\eta/2\sqrt{\tau}}^{\infty} \operatorname{erfc} \zeta d\zeta \\ & - \exp[-\eta/2(\beta+1)] \left[\tau - \left(\frac{\beta}{\beta+1}\right) \right. \\ & \quad \left. \times \frac{4\tau^{3/2}}{3\sqrt{\pi}} \right] + \dots \end{aligned} \quad (27)$$

An inverse solution for the temperature field corresponding to a constant value of $S_{\tau}^{(1)}$ and the corresponding value of the heat input function, may be obtained in a similar manner using equations (19) and (21). The results are

$$\begin{aligned} T^{(1)} &= \frac{S_{\tau}^{(1)} \exp[-\eta/2(\beta+1)]}{\beta+1} \left[\left(\tau + \frac{\eta^2}{2}\right) \right. \\ & \times \operatorname{erfc}\left(\frac{\eta}{2\sqrt{\tau}}\right) - \eta\sqrt{\left(\frac{\tau}{\pi}\right)} \exp(-\eta^2/4\tau) \\ & + \frac{\eta^{3/2}}{(\beta+1)^2} \int_{\eta/2\sqrt{\tau}}^{\infty} \operatorname{erfc} \zeta d\zeta - \\ & \quad \left. \tau \exp[-\eta/2(\beta+1) + \dots] \right] \end{aligned} \quad (28)$$

and

$$\begin{aligned} F^{(1)} &= S_{\tau}^{(1)} \left[1 + \frac{2\beta}{(\beta+1)} \sqrt{\left(\frac{\tau}{\pi}\right)} - \frac{\beta}{2(\beta+1)^2} \tau \right. \\ & \quad \left. + \frac{\beta}{6(\beta+1)^3} \frac{\tau^3}{\sqrt{\pi}} + O(\tau^{5/2}) \right]. \end{aligned} \quad (29)$$

In order to examine the manner in which the ξ -derivatives influence the solution, the expression for $F^{(2)}$ was found for the case when $S_{\tau}^{(1)}$ and $S_{\tau}^{(2)}$ are constant for $\tau > 0$. Using the technique already outlined in the preceding, the solution thus obtained is

$$\begin{aligned} F^{(2)} &= S_{\tau}^{(2)} + \frac{2\beta S_{\tau}^{(2)}}{\beta+1} \sqrt{\left(\frac{\tau}{\pi}\right)} - \frac{\beta S_{\tau}^{(2)}}{2(\beta+1)^2} \tau \\ & + \frac{4\beta}{3\sqrt{\pi}} \left[\frac{S_{\tau}^{(2)}}{8(\beta+1)^3} + S_{\xi\xi}^{(1)} \right] \end{aligned}$$

$$- \frac{1}{2} \left(\frac{S_{\tau}^{(1)2}}{(\beta+1)^2} + \frac{S_{\xi\xi}^{(1)}}{\beta+1} \right) \tau^{3/2} \dots \quad (30)$$

As expected, the second-order solution is similar in character to the first-order solution. Perhaps the most interesting aspect of this result is that the ξ -derivatives appear only in terms of order τ^4 .

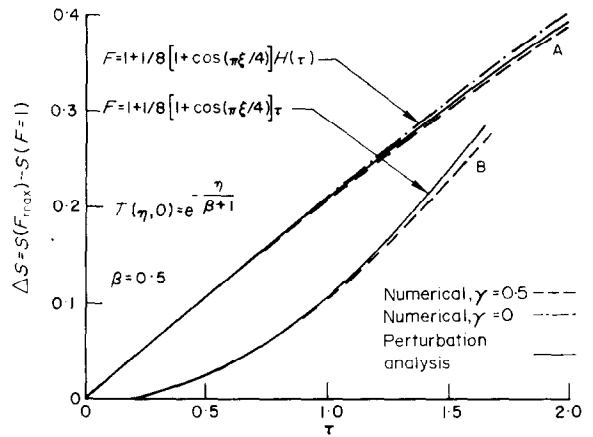


FIG. 2. Comparison of first-order analysis and numerical computation.

Figure 2 shows a comparison between calculations using the first-order solution to terms in τ^2 , [see equation (25)] and results of numerical integrations of the full equations. The calculations were performed for a sinusoidal heat input distribution to a two-dimensional conducting slab. In case A, the perturbation was applied as a step-function in τ , and in case B, the amplitude of the perturbation was a linear function of τ . In each case, a wavy surface developed, with the bottom of a groove corresponding to the maximum and a ridge to the minimum value of F . The ordinate ΔS , is the groove depth, or $S_{\max} - S_{\min}$. The value of the parameter β , which is the ratio of the energy absorbed in heating the material to the sublimation temperature to the heat of vaporization, is 0.5 for this example, and for all of the subsequent calculations. This value is representative of the larger values of β which would be encountered in physical situations.

Numerical results are shown for $\gamma = 0.5$ and for $\gamma = 0$ (no lateral conduction) for comparison with the predictions of the analysis. The range of validity of the time-expansion to τ^2 can be evaluated by comparing the results of the analysis with the numerical results for $\gamma = 0$. The use of the first-order solution is equivalent to assuming that the recession is locally one-dimensional and unsteady, corresponding to the local value of F . This situation is achieved in the numerical calculation by setting $\gamma = 0$. Lateral conduction effects during the initial time period considered may be evaluated by comparing the numerical results for $\gamma = 0$ and $\gamma = 0.5$.

IV. NUMERICAL METHOD

In order to obtain results in which effects of lateral conduction are of first-order importance, a numerical method of solution was constructed. The particular finite difference analog of the governing equations used here is an adaption of a method which was first employed by Clark

and Barakat [7] for a linear boundary value problem with stationary boundaries. The method uses a multi-level finite-difference representation of the differential equation, where the temperature is given by

$$T_{m,n}^j = \frac{1}{2}(U_{m,n}^j + V_{m,n}^j). \quad (31)$$

The superscript j refers to the time level, and the subscripts, m and n , identify the mesh point. The $U_{m,n}^j$ and $V_{m,n}^j$ each satisfies the complete difference equation and boundary conditions, but the calculations to determine $U_{m,n}^j$ begin at $m = n = 0$ and proceed in the direction of increasing m and n , and the calculations to determine $V_{m,n}^j$ begin at M, N , the maximum values of m and n , and proceed in the direction of decreasing m and n . The averaging of $U_{m,n}^j$ and $V_{m,n}^j$ to obtain $T_{m,n}^j$ is done in order to obtain a high level of accuracy. The finite-difference representations of the derivatives determine the stability properties of the system. Examples of difference equations of the U part of the temperature field are included here as follows:

$$\frac{\partial U}{\partial \tau} \cong \frac{U_{m,n}^{j+1} - U_{m,n}^j}{\Delta \tau}$$

$$\frac{\partial U}{\partial \eta} \cong \frac{1}{2} \left[\frac{U_{m,n+1}^j - U_{m,n}^j}{\Delta \eta_+} + \frac{U_{m,n}^{j+1} - U_{m,n-1}^{j+1}}{\Delta \eta_-} \right],$$

$$\frac{\partial^2 U}{\partial \eta^2} \cong \frac{2}{\Delta \eta_+ + \Delta \eta_-} \left[\frac{U_{m,n+1}^j - U_{m,n}^j}{\Delta \eta_+} - \frac{U_{m,n}^{j+1} - U_{m,n-1}^{j+1}}{\Delta \eta_-} \right],$$

and

$$\frac{\partial^2 U}{\partial \xi \partial \eta} \cong \frac{1}{4} \left[\frac{U_{m,n}^{j+1} - U_{m,n-1}^{j+1} - U_{m-1,n}^{j+1} + U_{m-1,n-1}^{j+1}}{\Delta \xi_- \Delta \eta_-} \right.$$

$$+ \frac{U_{m+1,n}^j - U_{m+1,n-1}^j - U_{m,n}^{j+1} + U_{m,n-1}^{j+1}}{\Delta \xi_+ \Delta \eta_-}$$

$$+ \frac{U_{m,n+1}^j - U_{m,n}^j - U_{m-1,n+1}^j + U_{m-1,n}^j}{\Delta \xi_- \Delta \eta_+}$$

$$\left. + \frac{U_{m+1,n+1}^j - U_{m+1,n}^j - U_{m,n+1}^j + U_{m,n}^j}{\Delta \xi_+ \Delta \eta_+} \right]. \quad (32)$$

The notation $\Delta\xi_+$ refers to the mesh spacing between m and $m + 1$; $\Delta\xi_-$ refers to the spacing between m and $m - 1$. The values of $\Delta\eta_+$ and $\Delta\eta_-$ are determined in the same manner. These expressions were substituted into the differential equation (9) and solved for $U_{m,n}^{j+1}$, explicitly. The space and time derivatives of the surface position were evaluated following the same scheme. The quantity S_m^{j+1} is computed from the boundary condition (11) at the time level j . In difference form, (11) becomes

$$S_m^{j+1} = S_m^j + \frac{\Delta\tau F_m^{j+1}}{(1 + \gamma^2 S_\xi^2)_m^j} + \beta \frac{\Delta\tau}{\Delta\eta_0} (T_{m,1}^j - T_{m,0}^j) - \frac{\beta\gamma^2 (S_\xi)_m^j}{(1 + \gamma^2 S_\xi^2)_m^j} \frac{\Delta\tau}{\Delta\xi_\pm} (T_{m\pm 1,0}^j - T_{m,0}^j). \quad (33)$$

The quantities $\Delta\xi_\pm$ and $T_{m\pm 1,0}^j$ are used depending on whether $S_\xi \leq 0$. The quantity $\Delta\eta_0$ is the vertical grid spacing between the surface ($n = 0$) and the first lattice point the body ($n = 1$).

Coupled with (33) is the phase change condition of (12) which, in difference form, becomes

$$S_m^{j+1} = S_m^j \quad \text{when} \quad T_{m,0}^j < 1 \quad (34)$$

and

$$S_m^{j+1} > S_m^j \quad \text{when} \quad T_{m,0}^j = 1.$$

Essentially the same finite difference approximation was used for the V part of the temperature field.

Two boundary conditions were investigated. For an insulated boundary at $m = 0$ and $m = M$ we require that the dependent variables be symmetric about the lateral positions $m = 0$ and $m = M$. For a body which is infinite in the lateral direction, the dependent variables are extrapolated parabolically. This is accomplished by writing

$$X_{-1,n}^j = X_{0,n}^j \left(1 + \frac{\Delta\xi_-}{\Delta\xi_+} \right) - X_{1,n}^j \frac{\Delta\xi_-}{\Delta\xi_+} \quad (35a)$$

along $m = 0$ and

$$X_{M+1,n}^j = X_{M,n}^j \left(1 + \frac{\Delta\xi_+}{\Delta\xi_-} \right) - X_{M-1,n}^j \frac{\Delta\xi_+}{\Delta\xi_-} \quad (35b)$$

along $m = M$, where X represents T or S . To satisfy the condition of infiniteness in the η direction the values of V at $n = N + 1$ are determined from (35b) where $\Delta\eta_+$ and $\Delta\eta_-$ replace $\Delta\xi_+$ and $\Delta\xi_-$, respectively. Additionally, in order to initiate the numerical calculation at any time step ($j + 1$), the boundary values U^{j+1} at $m = -1$ and V^{j+1} at $m = M + 1$ and also along $n = N + 1$ must be known. These quantities are obtained by extrapolating forward in time using the expression

$$X_{m,n}^{j+1} = 2X_{m,n}^j - X_{m,n}^{j-1}. \quad (36)$$

This computational procedure is explicit and unconditionally stable when applied to the conventional heat conduction equation, at least for several common types of boundary conditions [7]. The stability of the present method and of a more conventional explicit method (in which the time derivatives are approximated by a forward difference ratio and the space derivatives are approximated by central difference ratios evaluated at the previous time step) were studied by the method of Von Neumann, which is described by Richtmyer [8]. The choice of stable grid spacing and time step were found to depend upon γ , the surface recession velocity, surface slope, and surface curvature. Large values of any of these quantities would tend to cause instability. The maximum time step corresponding to stable computation for the conventional analog was predicted to be very small, implying prohibitively long computation times. The analysis indicated that the stability of the method of Clark and Barakat would be much less sensitive to the choice of time step, and that a substantially larger time step could be used with this method than could be used with the conventional one.

The finite difference formulation of the problem was programmed in Fortran IV, and computations were performed on the IBM 360 Model 75 and Model 91 of the UCLA Campus Computing Network.

Several one-dimensional, steady-state computations were made as check-out cases. With a

mesh spacing, $\Delta\eta$, of 0.1, a maximum η of 6.0, and time steps, $\Delta\tau$, of 0.00375–0.09, the computed value of the recession rate remained within 1 per cent of the exact solution for runs of 100–300 time steps. The error did not show a tendency to increase with time.

V. DISCUSSION OF RESULTS

The numerical program is very flexible and capable of accepting a wide variety of steady or unsteady heat flux distributions, arbitrary initial shapes of the ablating surface, and pre-heat conditions. The results presented herein pertain to a special situation which was selected because it illustrates the influence of lateral conduction on the problem in a relatively simple and straightforward manner.

In all cases the initial surface is flat and the temperature distribution in the (semi-infinite) slab corresponds to steady-state ablation under the influence of a uniform heat input ($F = 1$). These initial conditions exclude the transient period of preheating the surface up to ablation temperature. At time $t = 0$, the heat input is impulsively changed to a prescribed one-dimensional distribution and remains fixed thereafter. Thus the heating is steady (for $\tau > 0$) but spatially nonuniform, while the surface recession is, in general, both unsteady and nonuniform. The heat input function prescribes the energy input per unit projected area, not per unit actual area of the surface; as mentioned before, this situation corresponds to radiation.

Two heat input distributions were investigated. The first one is a cosinusoidal transition between two constant levels. Figure 3 shows a typical calculated history of recession of the ablating surface for a case in which $\gamma = 1$ compared to the case in which $\gamma = 0$ (no lateral conduction). The second heat input distribution is sinusoidal, for which typical surface recession histories are shown in Fig. 4. It is clear from these figures that an increase in lateral diffusion of heat results in smoothing out the shape of the receding surface.

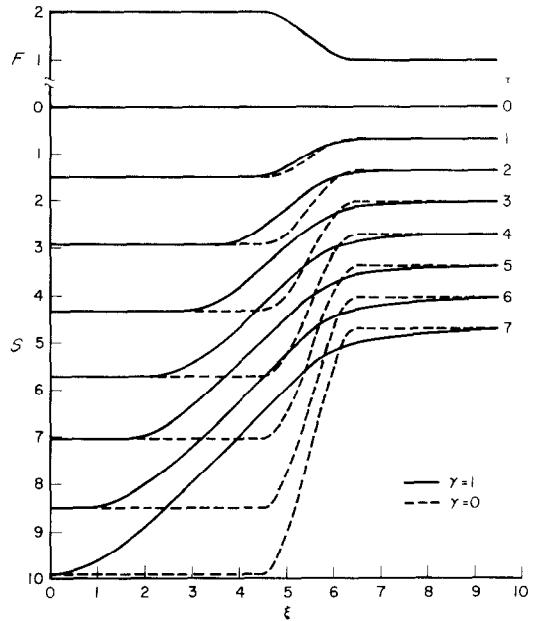


FIG. 3. Shape evolution of an infinite slab subjected to a two-level heat flux.

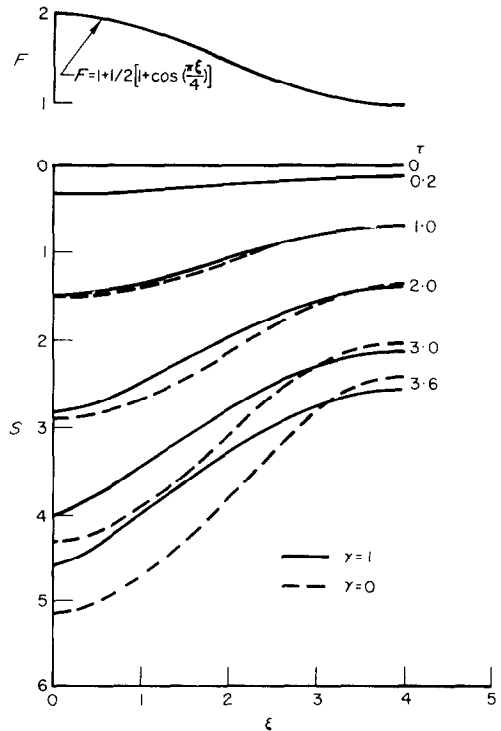


FIG. 4. Typical surface profiles, periodic heat flux.

The situation illustrated in Fig. 3 will be discussed first. The limiting cases can be stated: for $\gamma = 0$ (no lateral conduction) the surface must tend with time to an abrupt step; for $\gamma \rightarrow \infty$ the surface will tend to remain flat and recede uniformly at a rate corresponding to the average heat input ($F = 1.5$ in this case). For intermediate γ , the surface tends to the shape of a ramp which has a slope that appears to become constant. The maximum slope of the surface is plotted on Fig. 5 for this case and, incidentally, compared with results obtained by the use of the small-perturbation analysis.

The coordinates of Fig. 5 are scaled by certain parameters of the problem and suggest an empirical correlation of the form.

$$\frac{\gamma S_{\xi}}{\Delta F} \sim 1 - \exp(-\tau/\tau_0), \quad (37)$$

where

$$\tau_0 \sim \gamma^{-1}$$

This figure includes several calculations for different values of γ . The form of (37) suggests that other correlations may be obtained in which S_{ξ} is replaced by S , or a groove depth, ΔS .

The numerical results for $\gamma = 1$ also show that the ramp-like transition in the shape of the surface moves towards the regions of high heat input and the location of the "shoulder" remains nearly fixed (see Fig. 3). It follows that the total amount of mass ablated during the period represented by the calculation is considerably less than it would have been if there were no lateral conduction. This can be understood in terms of a more efficient utilization of the heat-sink capacity of the slab when the heat penetrating it can be distributed laterally. Figure 5 shows this by the difference function (\mathcal{S}) which is defined by

$$\mathcal{S} = \int [S(\gamma = 0) - S(\gamma)] d\xi. \quad (38)$$

It is normalized by the square of the approximate dimensionless step height which would result from ablation of a laterally nonconducting slab

$$H = \left[\frac{\Delta F}{1 + \beta} \right] \tau. \quad (39)$$

The approximation in this expression stems from the fact that equation (39) neglects the transient adjustment from the situation for $\tau < 0$ to the heat input function for $\tau > 0$.

These results suggest an apparently self-preserving evolution of the ramp-shape. How true similarity in the recession history is impossible if only on the grounds of overall energy conservation; if the surface recession were self-preserving, then the temperature distribution within the solid would also be self-preserving, and δ would be constant in time. The heat transferred to the slab in the region of shape transition is contained in a layer of thickness δ and, therefore is characterized by the product $H\delta$. H grows linearly with τ , so that the amount of energy stored in the solid sink increases linearly with τ . The mass deficiency, \mathcal{S} , is proportional to H^2 . Therefore, the difference between the total energy stored in the slab and that which can be stored in a self-preserving temperature field grows as τ^2 .

We are forced to consider the apparent self-similarity as an approximate characteristic of the history of the evolution of the surface. It seems that from an engineering standpoint this information is useful, especially in view of the remarkable accuracy of this approximation during a reasonably significant interval—throughout the following discussion we take this attitude.

The periodic heat input (typical example shown on Fig. 3) exhibits the same general trend. Figure 6 is a plot of groove depth vs. time; an insert in this figure shows the shape of the "groove" after it has reached the apparently stable depth. This shape is then also remarkably stable so that over intervals of, typically, 10τ the variation is within the plotting accuracy.

An interesting feature of the groove shapes is the development of a much smaller radius of curvature near the point of maximum heat input than at the point of minimum heat input. It is clear that this characteristic is necessary if a stable shape is to occur, since the existence of a stable surface requires that a large portion of the

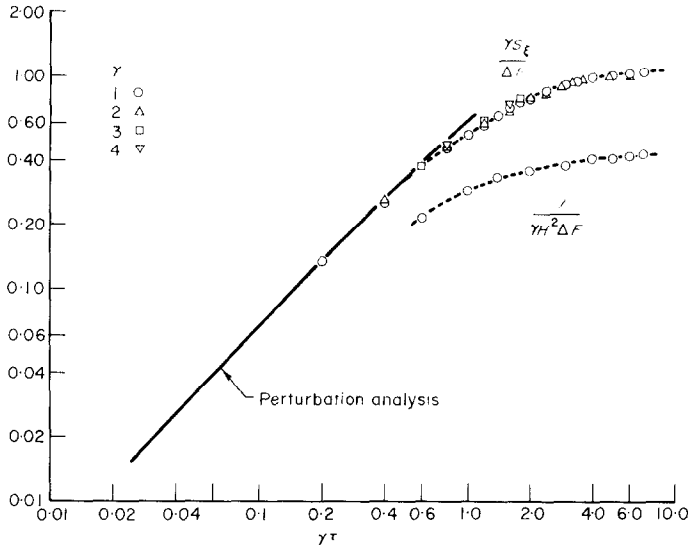


FIG. 5. Slope and mass-loss functions; infinite slab.

heat which is received near the region of maximum heat flux must be conducted laterally so that the recession rate where the heat flux is smaller can be increased. This, in turn, requires temperature contours to have relatively small

radii of curvature in the region of maximum F . Since the surface is an isotherm, its radius of curvature must be small in that region.

The case corresponding to $\gamma = 1.0$ and $F_{max} = 1.25$ was studied rather extensively. The same stable shape was achieved with two substantially different starting conditions (see Fig. 6), one which consisted of a flat initial surface and an initial temperature distribution corresponding to steady-state recession with $F = 1$, and another which was a curved surface having a considerably greater radius of curvature at $\xi = 0$ than the stable shape and an initial temperature distribution corresponding to steady-state recession at the local value of F . Also, calculations were performed with mesh spacing and time steps varying by a factor of 2, and resulted in differences of approximately 2 per cent in the depth of the groove.

A certain number of calculations resulted in numerical instability in the region of the bottom of the groove. This occurred for large values of γ and deep grooves (large $\mathcal{S}F/\gamma$); studies of the stability problem confirm that the stability criterion depends on the product of γ^2 and the surface curvature and slope. Figure 6 includes

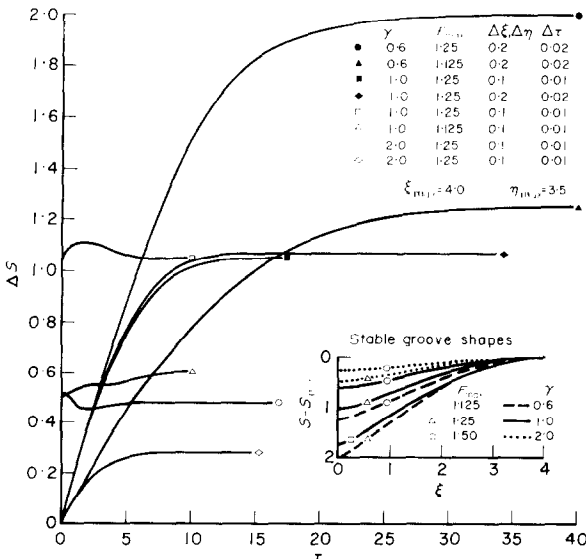


FIG. 6. Stable groove shapes; groove depth histories and final forms.

only data for which no difficulty was encountered; Fig. 7 gives this data and also data for a number of cases where the calculation proceeded only partly to the development of a quasi-stable groove before they had to be interrupted. For these cases we plot the time-evolution of the maximum slope and depth of the groove-like depression, again using the observed empirical generalization expressed by equation (37).

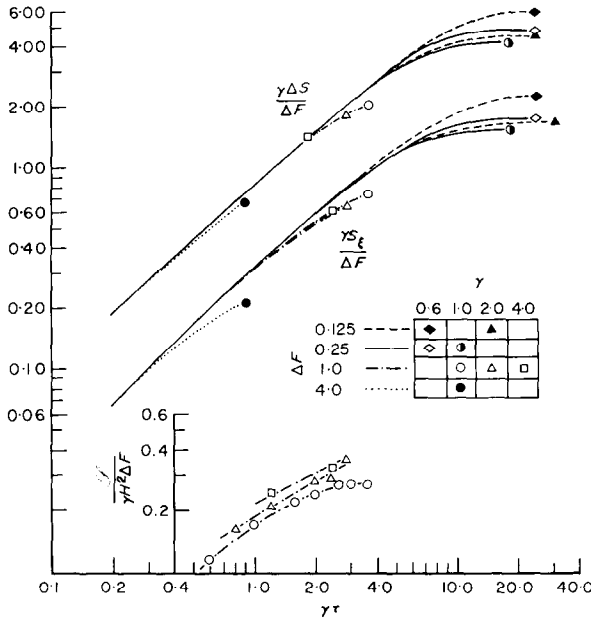


FIG. 7. Correlation of slope, groove depth, and mass-loss function, periodic heat flux.

Figure 7 also shows the mass-loss function, \mathcal{S} , for the periodic heat input and relatively short times. For sufficiently small values of time, a periodic heat input also results in a substantially smaller mass-loss due to ablation when lateral conduction is permitted. The long time results show that the quasi-stable groove recedes with approximately the recession rate corresponding to the mean heat input (within 3 per cent). To this level of accuracy the overall energy conservation conditions do not contradict the possibility of developing a self-preserving state in this case.

VI. CONCLUSIONS

The results presented here illustrate the effects of lateral diffusion in the solid on the evolution of the shape of its surface when it vaporizes, under the action of a spatially nonuniform, steady, radiant heating. Two typical distributions of heating were studied which are characteristic of situations encountered in practice.

Diffusion of heat tends to redistribute the energy required to preheat the solid to sublimation temperature in such a way that the gradients in the rate of sublimation of the surface are smoothed out relative to the local gradients of the heat input. In consequence, the shape of the subliming surface is always smoother than if lateral conduction were neglected (the locally one-dimensional approximation). There appears to be a tendency towards the development of an equilibrium, whereupon the shape of the surface remains constant to engineering accuracy. An empirical correlation of these results was proposed, and shown to hold remarkably well over a relatively wide range of the variables. The characteristic time-constant of the phenomenon is the product of the characteristic depth of the thermal layer in the subliming body and the characteristic length describing the spatial variation in the heat input divided by the thermal diffusivity of the solid. This form implies that both lengths are of equal importance. The amount by which the surface receded at a fixed value of the characteristic time is proportional to the length scale and to the magnitude of the heat flux nonuniformity. This functional form should provide a framework for the correlation of experimental data.

A different view of the observed phenomenon is this. If a given total heat input is distributed nonuniformly over the surface, lateral conduction results in a more efficient utilization of the heat-sink capacity of the solid and, at least during an initial period which is long relative to many practical situations, the total mass of ablated material is significantly less than if the same total heating were applied uniformly over the surface. Note that a two-dimensional non-

uniformity of heating in time and space (which was not explicitly studied here) would amplify this difference. These findings have interesting consequences in relation to many problems. For example, one problem which stimulated this research is the melting of ice fields under the influence of solar heating.

At small times, the surface recession rate is determined by the local value of the heat flux. The perturbation analysis provides an approximate method for computing the surface shape in this regime, the limits of which are indicated in part by comparisons between results of the analysis and numerical computations.

It also shows that a heat flux perturbation initially produces a recession rate which is greater than that corresponding to the new total heat flux.

ACKNOWLEDGEMENTS

This work was supported by NASA, and by the Campus

Computing Network, University of California, Los Angeles.

REFERENCES

1. H. S. CARSLAW and J. C. JAEGER, *Conduction of Heat in Solids*, 2nd edn, Ch. 11. Clarendon Press, London (1959).
2. J. C. MUEHLBAUER and J. E. SUNDERLAND, Heat conduction with freezing and melting, *Appl. Mech. Rev.* **18**, 951-959 (1965).
3. B. A. BOLEY, High temperature structures and materials, *Proc. Third Symp. Naval Structural Mech.*, p. 260. Pergamon Press, London (1963).
4. S. B. BANKOFF, Heat conduction or diffusion with change of phase, *Advances in Chemical Engineering*, edited by T. B. DREW *et al.*, Vol. 5. Academic Press, New York (1964).
5. D. L. SIKARSKIE and B. A. BOLEY, The solution of a class of two-dimensional melting and solidification problems, *Int. J. Solids Structures* **1**, 207-234 (1965).
6. H. G. LANDAU, Heat conduction in a melting solid, *Q. Appl. Math.* **8**, 81-94 (1950).
7. J. A. CLARK and H. Z. BARAKAT, On the solution of the diffusion equations by numerical methods, *J. Heat Transfer* **88**, 421-427 (1966).
8. R. D. RICHTMYER, *Difference Methods for Initial Value Problems*. Interscience, London (1957).

EVOLUTION DE FORME D'UNE SURFACE SUBLIMANTE SOUMISE À UN FLUX THERMIQUE INSTABLE ET SPACIALEMENT NON UNIFORME

Résumé—Une étude comprenant une analyse des perturbations et des calculs numériques, a été menée sur la conduction thermique bidimensionnelle et instationnaire dans un solide subissant un changement de phase sur une face exposée. La solution d'ordre zéro à partir de laquelle est développée la méthode des perturbations est la récession stable monodimensionnelle d'une plaque solide en réponse à un flux de chaleur uniforme. L'analyse a été faite pour des petites valeurs de $(\delta/b)^2$ où δ est la longueur caractéristique de la distribution de température dans le solide et b l'échelle de longueur de la non-uniformité latérale du flux thermique.

Une résolution analogue à celle des différences finies appliquée aux équations du problème est programmée, pour obtenir les résultats relatifs à une large non-uniformité dans le flux de chaleur et dans la forme de la surface. Des résultats sont présentés à titre d'exemple pour deux types d'alimentation thermique: (a) l'un dans lequel la variation spatiale est sinusoïdale et (b) l'autre qui consiste en deux niveaux constants connectés par une transition en demi-onde cosinus. On obtient un bon accord entre les prédictions de l'analyse de premier ordre et les résultats du calcul numérique pour des temps courts. Pour des valeurs du temps relativement grandes on trouve que les formes de surface calculées tendent à se conserver elles-mêmes. Dans le cas (a) les formes en relief tendent à être indépendantes du temps, et dans le cas (b) il y a une évolution vers une rampe rectiligne de pente constante. On trouve que la perte de masse du solide est plus petite quand la plaque est soumise à un échauffement spatialement non-uniforme que lorsqu'elle est chauffée uniformément avec la même intensité moyenne (quand la conduction latérale n'est pas négligée).

Pour un échauffement donné, la perte de masse avec conduction latérale est toujours moindre que lorsque la conduction latérale est négligée. Une corrélation empirique des résultats numériques montre que les pentes de surface et les profondeurs des sillons sont proportionnels à une échelle de longueur qui est associée à la non-uniformité du flux thermique et à sa valeur. Le temps caractéristique pour l'apparition des formes superficielles s'écrit $(\delta b/\alpha)$, où α est la diffusivité thermique du solide.

FORMÄNDERUNG EINER SUBLIMIERENDEN FLÄCHE

Zusammenfassung—Es wurde eine Untersuchung der zweidimensionalen unstationären Wärmeleitung in einem Feststoff mit Phasenänderung an den freien Oberflächen durchgeführt, und eine Störanalyse und

zahlenmässige Berechnungen gemacht. Die Lösung nullter Ordnung, aus der die Störanalyse entwickelt wurde, liefert ein stetig eindimensionales Zurückweichen einer Feststoffplatte als Reaktion auf eine gleichförmige Wärmezufuhr. Die Analyse wurde für kleine Werte $(\delta/b)^2$ durchgeführt, wobei δ die charakteristische Länge für die Temperaturverteilung im Feststoff ist und b ein Längenmass für die später ungleichförmige Wärmestromdichte. Die bestimmenden Gleichungen werden nach einer Analogie der endlichen Differenzen programmiert, um die Ergebnisse für eine grosse Ungleichförmigkeit von Wärmestromdichte und Flächenform zu erhalten. Musterergebnisse werden für zwei Arten der Wärmezufuhr gegeben; (a) für sinusförmige, räumliche Verteilung, und b, für zwei konstante Niveaus verbunden durch einen halben Kosinusbogen. Gute Übereinstimmung ergab sich zwischen den analytischen Rechnungen erster Ordnung und der numerischen Bestimmung für kleine Zeiten. Bei relativ langen Zeiten fand man, dass die berechneten Flächenformen selbsterhaltend wurden. Im Fall (a) wurden Rillenform und Rillentiefe zeitunabhängig, im Fall (b) ergab sich eine Gerade mit konstanter Steigung. Der Massenverlust des Feststoffs wurde kleiner, wenn die Platte einer räumlich ungleichförmigen Beheizung ausgesetzt war, als bei gleichförmiger Beheizung mit derselben mittleren Intensität (wenn man die spätere Wärmeleitung nicht vernachlässigt). Bei gegebener Beheizung war der Massenverlust mit seitlicher Ableitung immer kleiner als ohne deren Berücksichtigung.

Eine empirische Beziehung für die zahlenmässigen Ergebnisse zeigt, dass die Steigung der Fläche oder die Rillentiefe einem Längenmass proportional sind, das auf die Ungleichförmigkeit und die Grösse der Wärmestromdichte bezogen ist. Die charakteristische Zeit für das Auftreten einer Flächenveränderung ist $(\delta b)^2/\alpha$, wobei α die Temperaturleitzahl des Feststoffs ist.

РАЗВИТИЕ ФОРМЫ СУБЛИМИРУЮЩЕЙ ПОВЕРХНОСТИ ПОД ДЕЙСТВИЕМ НЕСТАЦИОНАРНОГО ПРОСТРАНСТВЕННО НЕОДНОРОДНОГО ТЕПЛОВОГО ПОТОКА

Аннотация—Проводилось исследование двумерной нестационарной теплопроводности в твердом теле при фазовом изменении на границе, включая анализ разложения в ряды и численные расчеты. Нулевой член разложений в ряды описывает установившееся однородное углубление твердой пластины под действием однородного подвода тепла. Этот анализ проведен для небольших значений $(\delta/b)^2$, где δ —характеристическая длина для профиля температуры в твердом теле, а b —шкала длины продольной неоднородности теплового потока.

С целью получения результатов для большой неоднородности как в тепловом потоке, так и в форме поверхности запрограммирован конечно-разностный аналог исходной системы уравнений. Представлены результаты для двух видов подвода тепла: (а) по синусоиде и (б) по двум прямым, сопряженным полупериодом косинусоиды. В случае малых времен получено хорошее соответствие между аналитическим решением первого приближения и численными результатами. Для относительно больших значений времени найдено, что рассчитанные формы поверхности самосохраняются. В случае (а) рельефные формы и глубины стремятся стать независимыми от времени, а в случае (б) наблюдается тенденция к образованию прямой линии постоянного уклона. Найдено, что потеря массы твердого тела меньше, когда пластина подвержена пространственно неоднородному нагреву, чем если она нагревается однородно с одной и той же средней интенсивностью (если продольная теплопроводность не игнорируется). При данном нагреве потеря массы при продольной теплопроводности всегда меньше, чем если продольная теплопроводность не учитывается.

Эмпирическая корреляция числовых расчетов показывает, что наклоны поверхности или глубины рельефов пропорциональны шкале длины, связанной с неоднородностью теплового потока и его величиной. $(\delta b)^2/\alpha$ является характеристическим временем при появлении очертаний поверхности, α —температуропроводность твердого тела.